Iraqi Geological Journal

Journal homepage: https://www.igj-iraq.org

Cloud-Based Computational Model for Direct Surface Runoff Estimation Using Remote Sensing in Arid and Semi-Arid Regions

Rania A. Saeed[1*], Ashraf M. Elmoustafa[2], Sherien A. Zahran[3] and Morad H. Abdel-Daem[2]

[1] Planning Sector, Ministry of Water Resources &Irrigation, Cairo, Egypt
[2] Irrigation & Hydraulics Department, Faculty of Engineering, Ain Shams University, Cairo, Egypt
[3] Environment and Climate Change Research Institute, National Water Resources Center and High Institute of Engineering & Technology, Al Obour, Cairo, Egypt
[*] **Correspondence:** 1901882@eng.asu.edu.eg

Received:
22 March 2025
Accepted:
15 May 2025
Published:
31 July 2025

Abstract

Accurate surface runoff evaluation stands critical for hydrological studies and both water resource governance and flood danger assessment together with land-use design. The current methods of runoff measurement depend on in situ data sources, although the limitations in data accessibility and availability and operational expenditure. Rainfall-runoff estimation is a difficult task in unmeasured basins because these areas lack essential devices for data collection, such as stream gauges. Water resource assessment alongside flood prediction becomes challenging because ungauged basins are extensively spread across the Earth's surface. Water availability decisions, together with flood control and sustainable water management, face challenges because rainfall-runoff models remain unspecified. The research develops a Cloud-Based Computational Model, which incorporates remote sensing data and the Natural Resources Conservation Service Curve Number method to calculate direct surface runoff. The research examines arid and semi-arid regions, taking the Tekeze-Atbra sub-basin in Sudan as a case study, which is a significant tributary of the Nile River that experiences substantial runoff variations between seasons. The model incorporates satellite data (rainfall, LULC, soil moisture, and DEM) to estimate runoff while providing better spatial accuracy. The model demonstrates enhanced performance through evaluation testing that checks observed hydrological data and validates its effectiveness in offering better real-time water management predictions. The model demonstrated reliable results through runoff assessments against hydrological records spanning from 2015 to 2020, thus proving itself as a flexible computing technique for forecasting runoff linking remote sensing approaches with cloud computing features and hydrological modeling systems to handle data-sparse regions.

Keywords: Rainfall runoff; NRCS-CN; RS; Cloud-computing; Tekeze- Atbra:Sudan

1. Introduction

Water resource management and flood forecasting, together with sustainable agricultural planning, depend on precise direct surface runoff predictions, particularly in water-scarce, arid, and semi-arid areas. Runoff estimation through standard methods depends on on-site measurements yet proves to be slow and expensive as well as suffering from spatial constraints. Hydrological models are used to estimate runoff and predict extreme events (floods and droughts). In particular, hydrological models are beneficial to simulate rainfall runoff process for a comprehensive understanding of hydrology and runoff

formation mechanisms of a catchment (Ashenafi et al., 2023). These models range from simple empirical techniques to complex physically-based simulations (Hans et al., 2000).

The scarcity of well-distributed meteorological stations together with sparse station density creates obstacles to obtaining accurate surface runoff data in these regions. The current system restricts the correct registration of environmental variables, which limits researchers from characterizing both spatial and temporal patterns needed to create water management strategic plans and conduct research.

The use of distributed models also has several benefits owing to their ability to mimic both temporal progression and spatial heterogeneity within a watershed. An important advantage of the grid-based distributed models is the ability to mirror heterogeneity in the rainfall pattern and catchment characteristics at the pixel level, which may make them more appropriate for providing better flood hydrograph reproduction.(El-Bendary, 2019). Additionally,The grid-based approach is a topic of ongoing study, driven by the availability of high-resolution datasets, advancements in GIS and remote sensing techniques, and the growing power of modern hardware and software (Paudel, 2010).

The combination of RS products with cloud-based computation created a disruptive solution that performs big-scale, real-time hydrological evaluations and does so efficiently and with financial advantages (Babita Pal, 2011). The Natural Resources Conservation Service Curve Number (NRCS-CN) method serves as the main empirical approach to predict surface runoff, while this work creates and implements a cloud-based computational tool for runoff assessment.

According to Zhang (2019) the use of single CN values from traditional NRCS-CN falls short for accurate runoff modeling and grid-based CN modeling provided better results in Taiwan's Chenyoulan watershed (Zhang, 2019). The research Ajmal et al. (2016) of developed slope-adjusted CN values specifically for mountainous regions which enhanced the accuracy of 39 South Korean watersheds (Ajmal et al., 2016).

The research by Afkril et al. (2020) developed a grid cell-based runoff routing system through the combination of CN and rainfall data which resulted in high model efficiency rates (NSE > 0.75) when applied to Indonesian catchments. Hydrograph simulation depends strongly on spatial distribution according to this study (Afkril et al., 2020).

The CN-GIS approach in semi-arid mountainous regions of Iran delivered accuracy at a moderate level amounting to ~55% (Ebrahimian, 2012).

Gupta et al. (2022) applied GIS-based NRCS-CN methodology to measure runoff across 63 sub-basins in Assam, India. Modified curve numbers (CNs) for land utilization, soil classifications, and topography. The model produced dependable simulations for water resource planning because it verified observed runoff using excellent correlations ($R^2 \geq 0.8$) (Gupta et al., 2022).

Kencanawati et al. (2024) developed an empirical NRCS-CN model for unmeasured catchments through classification of local soils and infiltration testing which lead to accurate run-off predictions from CN optimization and spatial data integration (Kencanawati et al., 2024).

One of the most critical difficult challenges is the ability to estimate rainfall and runoff relationships in unmeasured basins, where no data collection devices, including stream gauges are installed. These ungauged basins occupy a major part of the earth's surface, especially in the developing world, and hence a proper assessment of water resources and flood potentials cannot be made. Various challenges in practice are encountered related to decision making for estimating available water, flood protection measures and sustainable water use management since definitive rainfall–runoff models are lacking.

The proposed research objective is to construct a cloud-based computational model (CBCM) distributed hydrological model that directly calculates runoff at a basin scale using the NRCS-CN method. The research also aims for CBCM to be applicable within different basin scales with different RS products, allowing better anticipation and management of water resources while considering spatial and environmental context.

2. Study Area

2.1. Study Area Location

The Atbra River serves as the Nile's final tributary by flowing into the main river 322 km north of Khartoum, Sudan. The river begins in Ethiopia at heights ranging from 1,830 to 3,000 m in the area surrounding Lake Tana, which lies approximately 50 km north.Similar to the Blue Nile, the Atbara River undergoes a quick descent, which transforms it into an enormous sediment-filled waterway during times of flood while it condenses into several detached pools in drought seasons. The computed annual discharge rates stand at 12 billion m^3 (BCM) and create 12% of the total inflow at Aswan. The Tekeze-Atbara sub-basin has a total surface area of 23.51 thousand km^2 (Akol et al., 2016). **Error! Reference source not found.** shows the location of the Tekeze Atbra sub-basin.

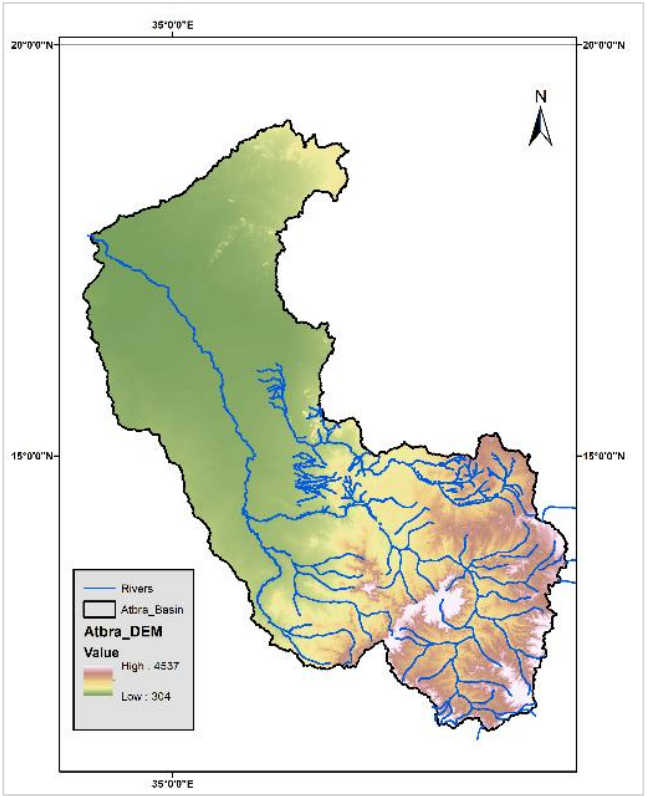


Fig. 1. Tekeze Atbra sub-basin location

2.2. Climate Conditions

The climate of Atbara River basin falls into semi-arid up to arid type and experiences most of its rainfall from June to September. The Ethiopian highlands determine most of the fluctuations that occur in the river's water flow because of their rainfall patterns. Research findings show that land-use and climate changes led to modifications in the way rainfall and streamflow occur both in space and time (Gebremicael et al., 2017). July and August mark the peak flood season across the upper portion of the sub-basin whereas the lower Sudan portion stays virtually rainless during the entire year.

The lower Atbara basin falls below 100 mm of annual rainfall therefore classifying it as a desert or semi-desert region where vegetation is scarce. Areas that maintain a high-water table present the main regions where vegetation can thrive. During rainy years this region turns into temporary open grazing land which the locals call Gizzu. Shrubs and dwarf trees grow at low to medium densities in this region as the annual rainfall stays between 50–100 mm. Fig. 2 shows the basin average monthly rainfall.

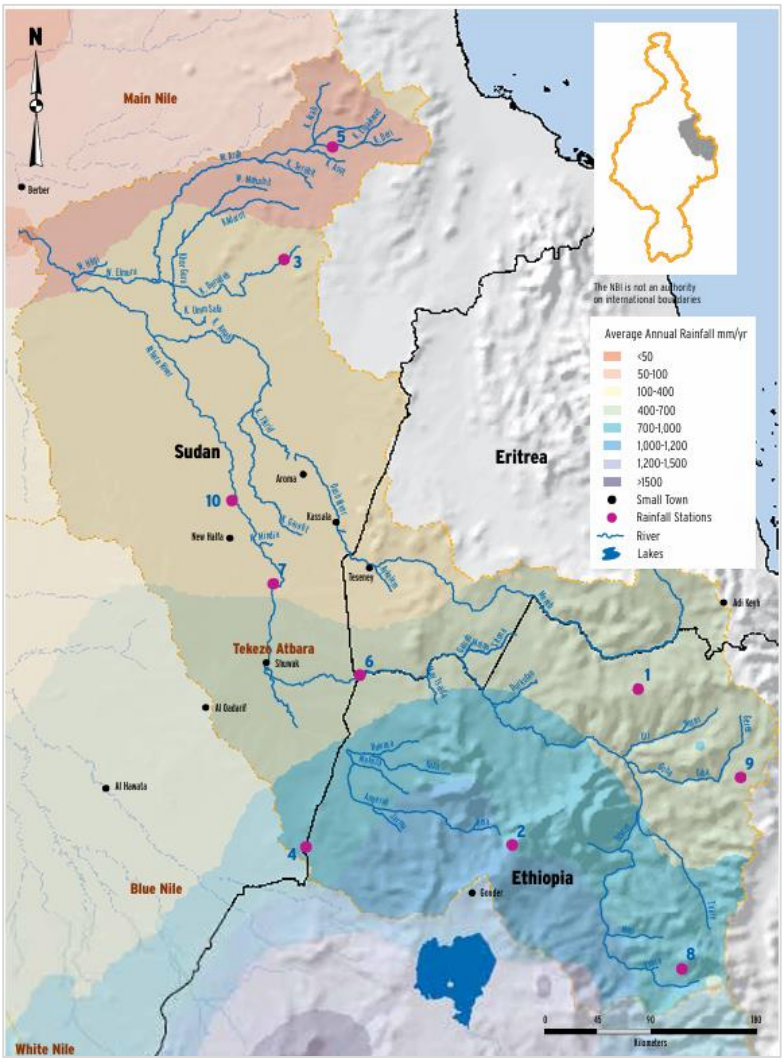


Fig. 2. Tekeze Atbra sub-basin average monthly rainfall (NBI, 2016)

TheAtbara has an annual maximum temperature of 35.75 degrees Celsius while April shows the highest peak of 39.68 degrees Celsius.Measures from both high and low temperature readings show statistically significant elevation which indicates a persistent rise in temperature throughout years.(El-Mahdy et al., 2024)

2.3. Land Cover

The Atbara basin for the period between 1972 and 2014 experienced over 72% of the land cover feature conversion from one category to another through human interference. The quantity of natural vegetation including forest land decreased substantially throughout the initial decades until the 1990s when watershed management initiatives improved its status (Gebremicael et al., 2017).

The Atbara basin's vegetation includes both herbs and shrubs and trees which reach maximum heights of 4 m. Rainfall patterns determine the annual growth cycle of most grasses that exist in the region. Intense grazing together with unreliable rainfall patterns create conditions where dry biomass cannot provide enough fuel to support fires annually during dry seasons. Plant growth during dry conditions and times of heavy grazing proves insufficient to establish enough vegetation in the region (Fischer et al., 2022). Fig. 3 shows the basin LULC classification.

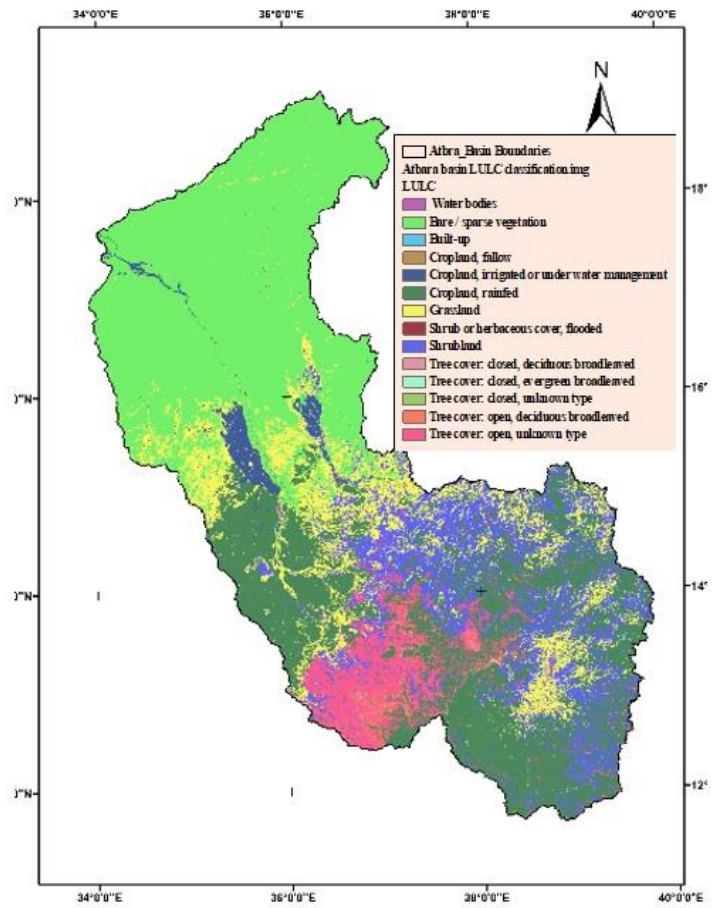


Fig. 3. Tekeze Atbra sub-basin LULC classification map

2.4. Soil Moisture

The Atbara Basin's environmental elements together with soil types determine the present levels of soil moisture which affect agricultural systems as well as hydrological systems. Non-fertile soil types in the region principally consist of Aridisols and Entisols whereas low rainfall results in poor natural water retention capacity. The water requirements for growing crops become extremely challenging due to these soils because irrigation remains the only viable solution. Aridisols exhibit argillic along with duric and salic moisture regimes whereas their sublayers contain salts and clays or carbonates that restrict water absorption. The proximity of Entisols located near floodplains makes them ideal for agricultural purposes because sedimentary processes enrich the soil quality and improve water retention capacities (El Abbas et al., 2017). Fig. 4 shows the basinsoil moisture classification map.

2.5. Hydrogeological Conditions

The Atbra Basin in eastern Sudan maintains a commercially viable alluvial aquifer that extends from Precambrian basement rocks up to sandstone and alluvial sediment formations. The groundwater measures between 11–40 m in depth while transmissivity varies from 1,000–1,500 m^2/day and storage amount to roughly 1.45 billion m^3. The primary water source for recharge at the Atbara Basin stems from the Atbara River which maintains steady flow approaching northwest. (Elsheikh et al., 2014)

Mohammednoor et al. (2023) Paleosol research shows that the aquifer received recharge during past periods of enhanced humidity.Data indicates that the aquifer demonstrates high resistance to seasonal changes (Mohammednoor et al., 2023).

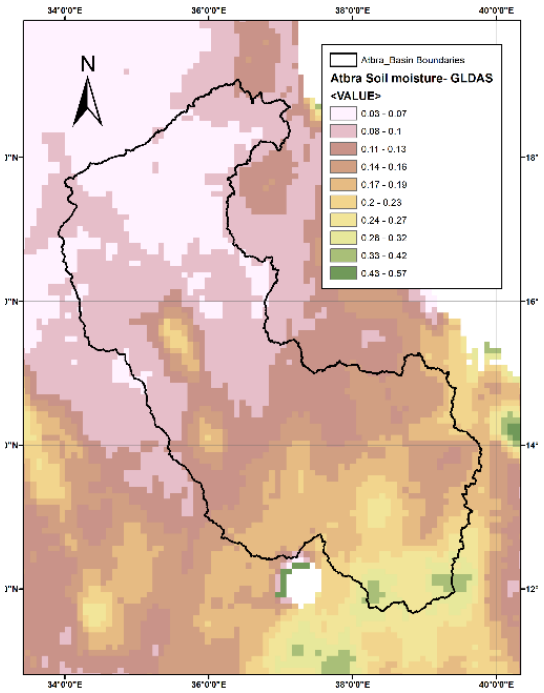


Fig. 4. Tekeze Atbara sub-basin soil moisture mapMaterials and Methods

2.6. NRCS-CN Method

The Soil Conservation Service, now known as the Natural Resources Conservation Service (NRCS), created the NRCS-CN method in 1954 and published it in 1956 as Section 4 Estimation of Direct Runoff from Storm Rainfall (National Engineering Handbook).

The conventional NRCS-CN approach is a lumped rainfall-runoff model that is event-based. It is founded on the combination of the equation for water balance (Miller, 1994).

The NRCS-CN model functions by measuring how rainfall affects the maximum water-holding capacity of an entire watershed. The method relies on a dimensionless curve number (CN) spanning between 0 to 100 to indicate the runoff risk in specific regions. Areas exhibiting higher CN values tend to produce more runoff because they lack sufficient infiltration yet areas with low CN values tend to have good infiltration rates.The Curve Number (CN) calculation integrates hydrologic soil groups (each group has varying infiltration capacities beginning with Group A through Group D).

The equation formula for NRCS-CN is as follows:

$P = Ia + F + Q$ (1)

P is total rainfall, Ia is initial abstraction, F is cumulative infiltration excluding Ia, and Q is direct surface runoff.

$\frac{Q}{(P-Ia)} = \frac{F}{S}$ (2)

And Ia = ʎS (3)

The most common form of the NRCS-CN method is given by Equations (1) and (2):

$Q = \frac{(P-Ia)^2}{(P-Ia+S)}$ For P > Ia

$Q = 0$ For P <= Ia

Q is direct surface runoff (mm), P is total rainfall (mm)

Ia is the initial abstraction (mm).

S is the potential maximum storage (mm), S = 254 (100 / CN − 1).

CN: (0–100) curve number (defined by land use and hydrological soil type)

The rainfall-runoff model incorporates data acquisition and transformation followed by precipitation modeling and water flow modeling and validation steps and analysis functions. Remote sensing data undergoes cross-comparison with gauge measurements to validate streamflow data before the model can be considered accurate. The model determines runoff through classification of rainfall together with soil type and slope characteristics. The final part delivers complete space-time patterns of runoff variations, which link land use and climate factors together with watershed attributes for useful hydrological management planning.

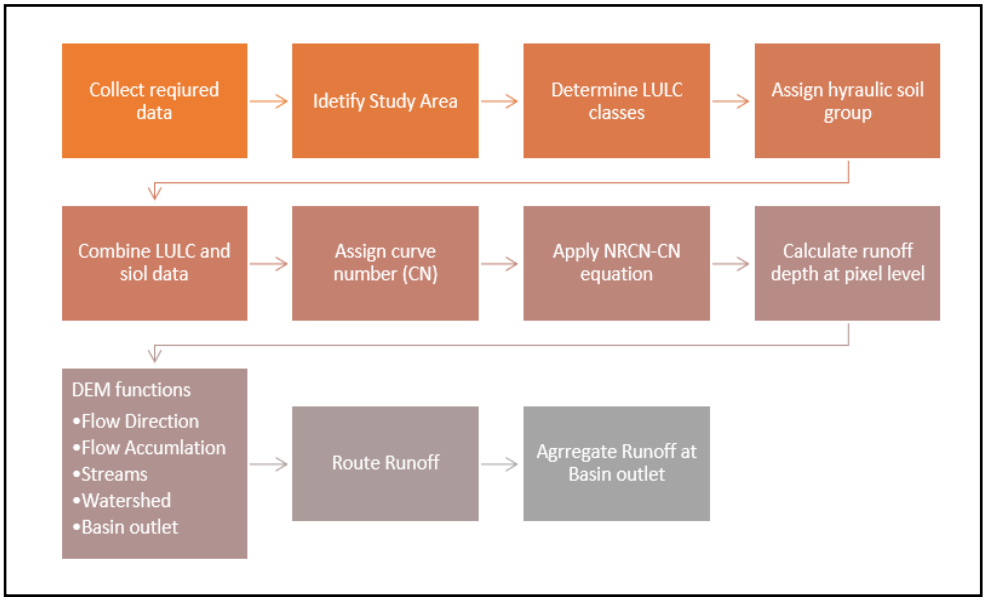


Fig. 5. Surface runoff estimation using NRCS-CN model procedures

The CN method from the NRCS, together with DEM functions, enables the estimation of runoff. The procedure begins by preparing LULC classifications with soil grouping and then merging these maps to extract CN values. The NRCS-CN equation, together with hydrological functions generated from the DEM, enables calculating pixel-level runoff depth. The combined runoff from individual cells follows a process that routes the water toward the basin outlet.

2.7. Data Sources

The observed precipitation data source is WMO meteorological stations. These data were downloaded from Northern Illinois University. Then downloaded data were decoded to extract the precipitation observation for each station.observed discharge data were collected at the Tekeze Atbra sub-basin outlet, Sudan. The observing station is located at Atbra km 3.0 by the basin outlet

Remote sensing data matrix used as model inputs to estimate direct surface runoff are shown inTable **1**.

Table 1. Remote sensing data matrix

2.8. Model Description

The proposed model combines Google Earth Engine with GIS Model Builder to calculate outlet runoff amounts throughout a step-by-step process. The steps are shown in **Error! Reference source not found.**.

1. Data preprocessing (Geographic Information System GIS model builder)

2. Model Calculation (Data analysis)- (Google Earth Engine GEE model)
3. Model Tools and Outputs- (GEE model)

The system operates across two main sections, as shown in Fig. 6. vGIS Model Builder: Handles spatial preprocessing of hydrological parameters, such as Curve Number (CN), potential maximum storage (S), and DEM-derived attributes. GEE Model: completes rainfall-runoff assessments alongside velocity determination and travel time simulations and runoff accumulation computations for the basin outlet.

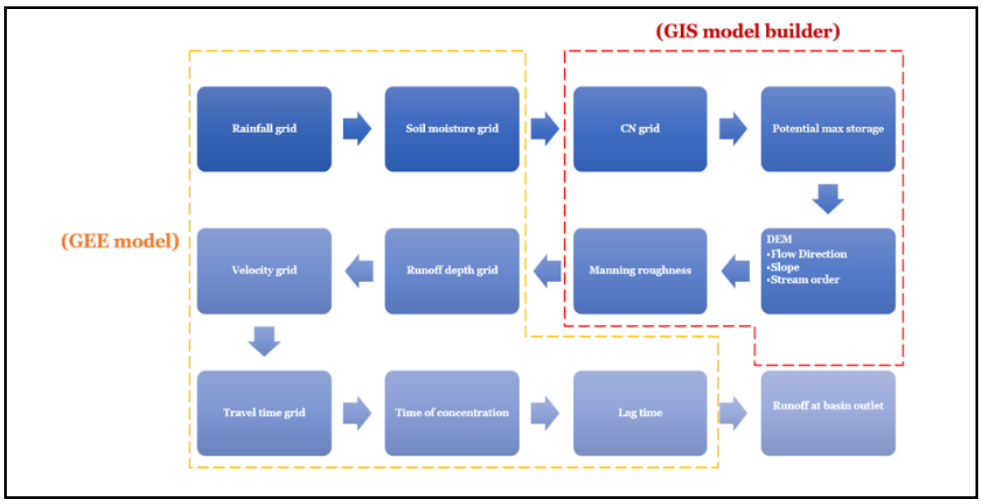


Fig. 6. The developed model systems flow chart

2.8.1. GIS model builder (hydrological preprocessing)

2.8.1.1. The (CN) grid

Exists as a calculated result between land use/land cover data and soil characteristics, which governs water infiltration and surface runoff as shown in Fig. 7.

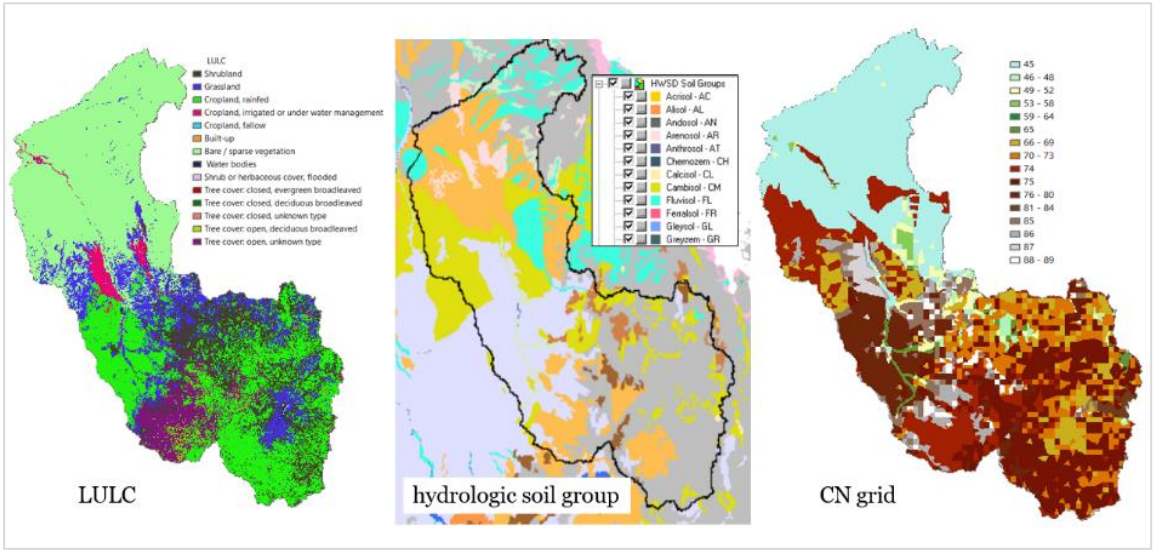


Fig. 7. The CN grid derivation using GIS model builder

2.8.1.2. Water retention capacity(S) grid

Relies on the computed Potential Maximum Storage (S) value from CN as shown in Fig. 8.

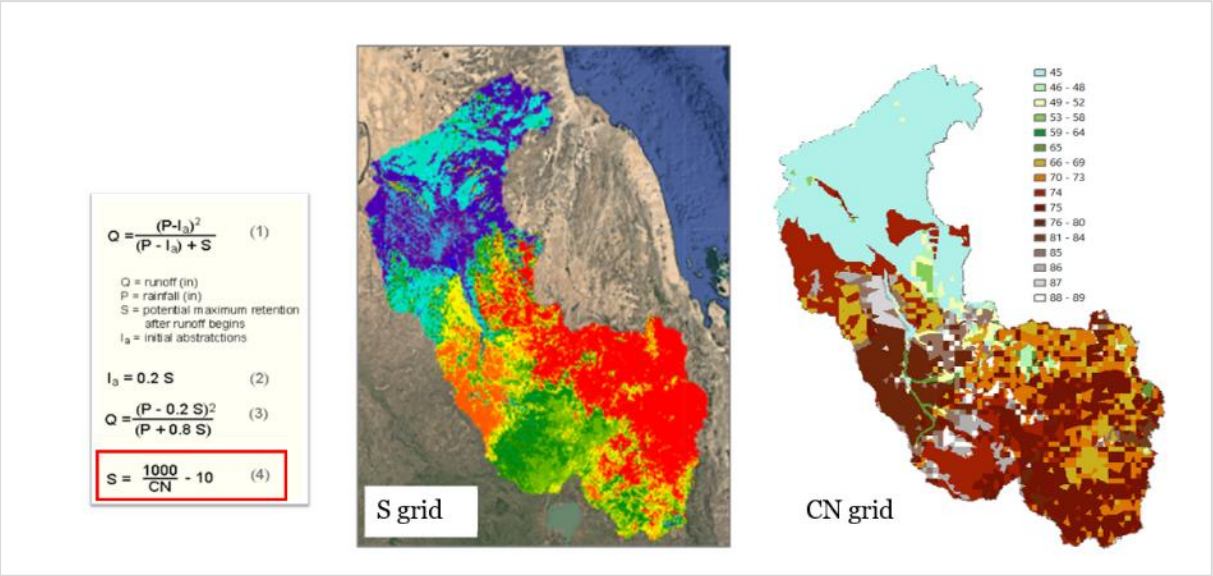


Fig. 8. The S grid derivation using GIS model builder

2.8.1.3. Manning's roughness coefficient

To create a Manning's roughness coefficient grid in a land cover raster attribute data table that associates land cover classes with Manning coefficients. Then the Reclassify tool (Spatial Analyst) was used in order to label each land cover class with Manning's coefficients and generate a raster dataset in which the cells contain roughness coefficients, as shown in Fig. 11.

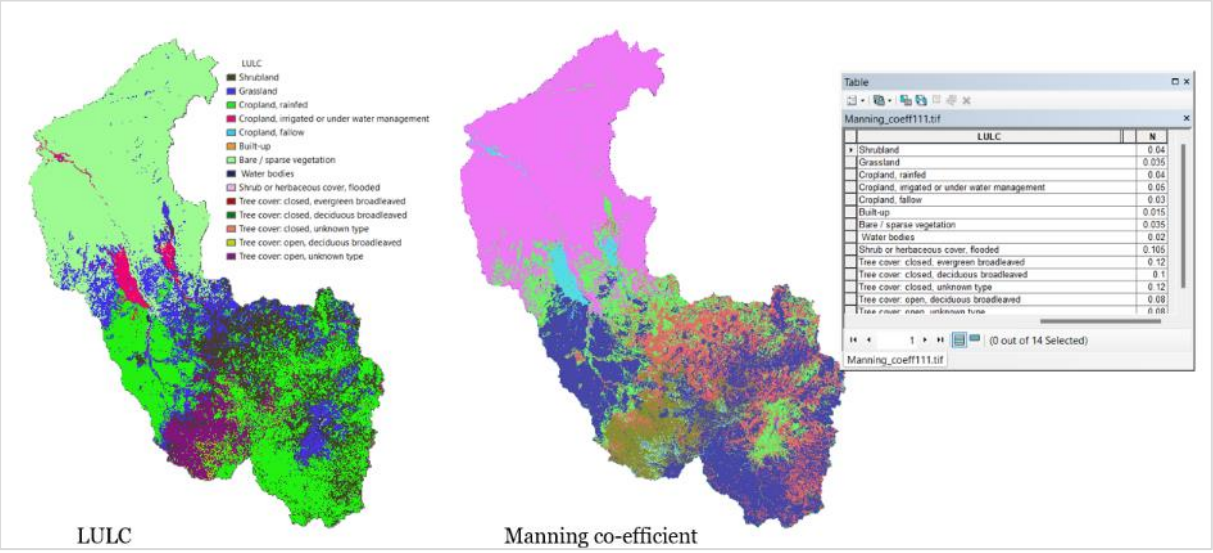


Fig. 9. The Manning's roughness coefficient grid derivation using GIS model builder

2.8.1.4. DEM processing

The process of DEM processing conducts multiple grid computations to track the water flow patterns across terrain surfaces as shown in Fig. 10. Water flow directions emerge from the Flow Direction Grid, which accretes elevation data to produce the Flow Accumulation Grid that links upstream cells together. The slope grid maintains essential control over water velocity because it determines how fast water moves, thereby affecting runoff rates. The Stream Order classification enables water flow tracking in watersheds through its drainage network.

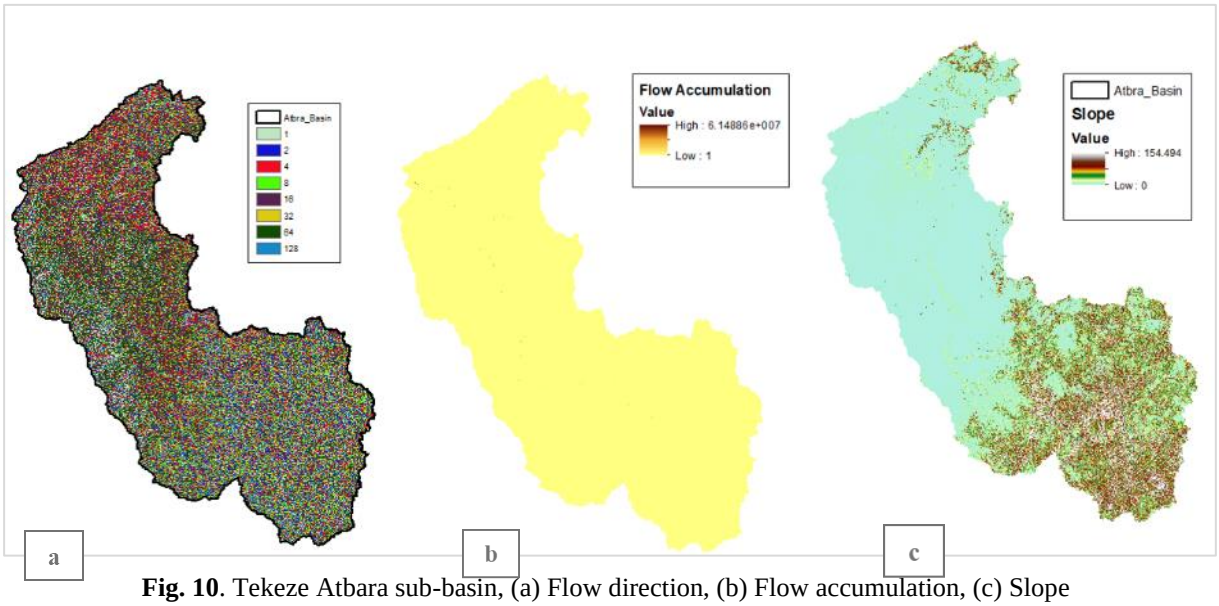


Fig. 10. Tekeze Atbara sub-basin, (a) Flow direction, (b) Flow accumulation, (c) Slope

2.8.2. GEE Model builder (rainfall-runoff calculation)

The GEE model uses the prepared layers for hydrological computations and remote sensing inputs to process dynamic runoff calculations. Fig. 11 shows the developed model user interface.

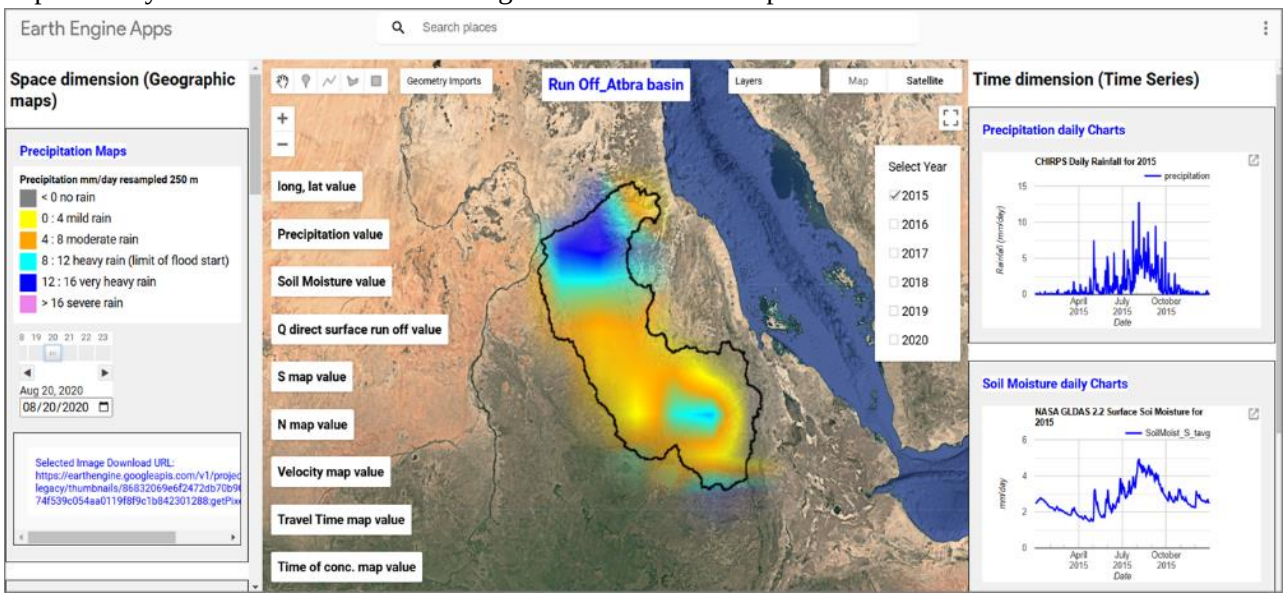


Fig. 11. The developed model user interface

The GEE model displays three main sections throughout the user interface which contain the code editor panel and the output panels and the console area. The code base includes a script for calculating various hydrological functions. Users can perform code input and editing and command execution through a logical structure found in the platform targeted for time series chart generation with RS data. The visual interface of the cloud computational program features a code editor that displays RS data. A time series charts is generated from selected years based on data processing done by the code. Users can select analysis years through a checkable box. Easy interpretation becomes possible through this layout which utilizes labels and colored-coded precipitation levels. Users can find a download link which provides the processed dataset.Fig. 12 shows the developed model python scripts code panel.

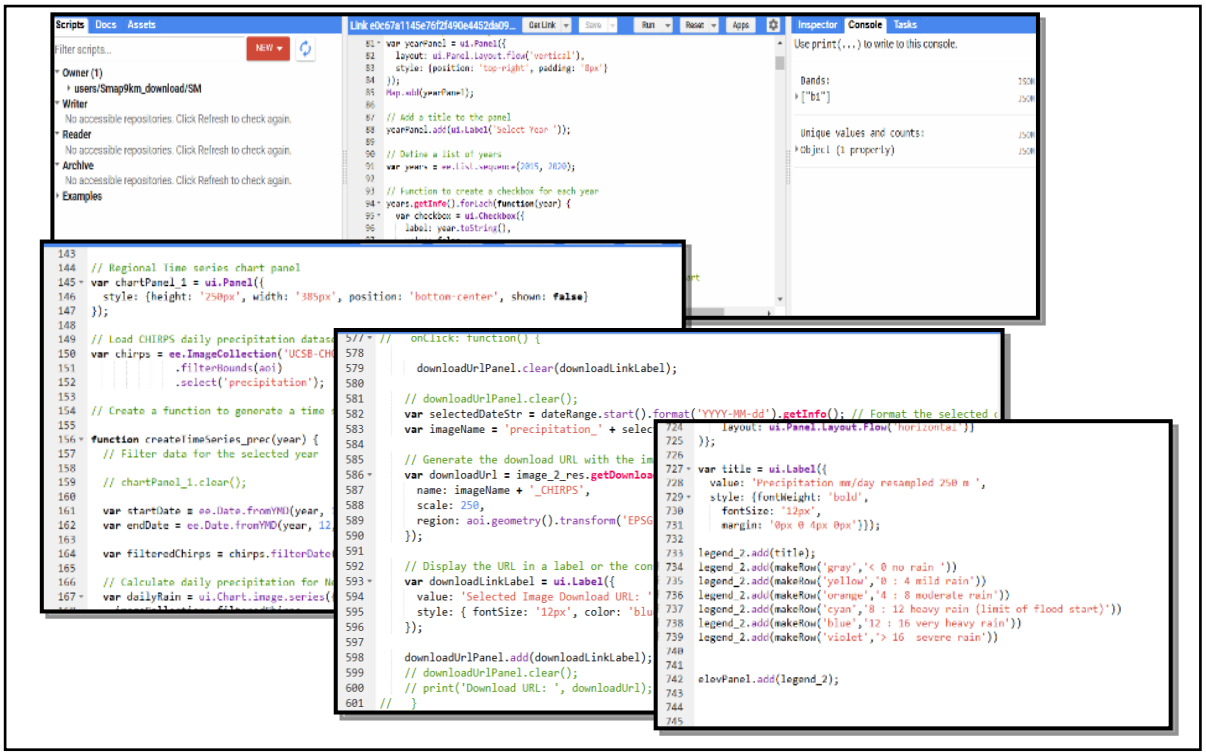


Fig. 12. The developed model python scripts code panel

2.8.2.1. Direct runoff depth grid

Derived on a daily basis using the NRCS-CN equation as shown in Fig. 13with the following inputs: 1. The precipitation data from CHIRPS provides the daily rainfall grid data. 2. The initial abstraction from the GLDAS soil moisture grid daily data, 3. CN grid derived from GIS Model Builder

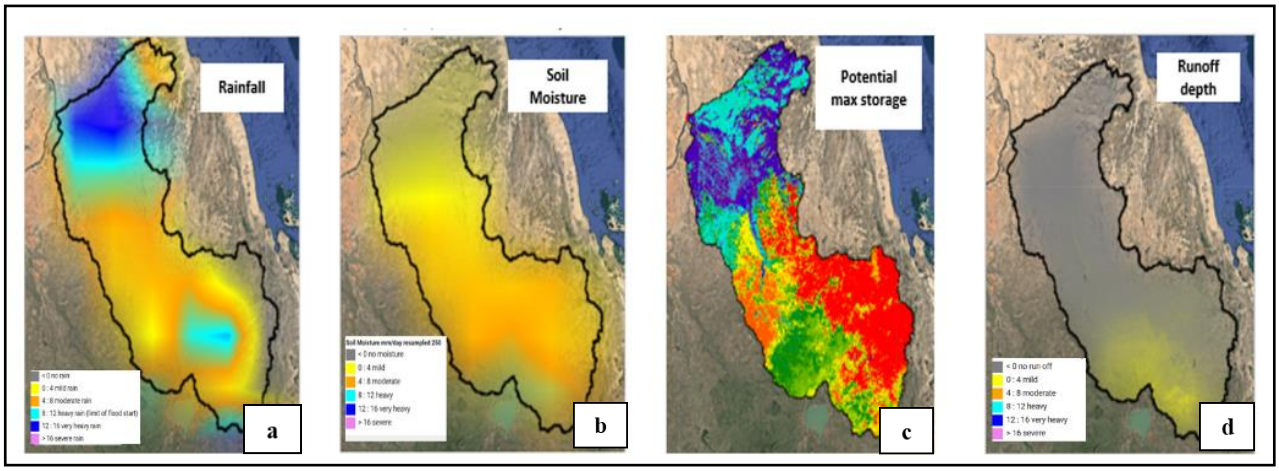


Fig. 13. Tekeze Atbara sub-basin, (a) rainfall, (b) soil moisture, (c) Potential max storage, (d)direct runoff depth

2.8.2.2. Velocity grid

Manning's roughness coefficient along with slope serves as inputs to create a velocity grid according to Manning's velocity equation (Jonathan, 2002).

$$V_i = \frac{1}{n_i} x R_i^{(2/3)} x \sqrt{S_i} \quad (1)$$

Vi = flow velocity, m/s.

ni = Manning's coefficient of roughness (dimensionless) - the measure of the resistance to flow offered by the surface roughness of the channel.

Si = longitudinal slope.

R = Hydraulic radius (m)

$$R = \frac{A}{P} \quad (2)$$

A= Area of flow in cross section (m2)

Area of flow in cross section: is the area of water flowing through the grid cell

$$A = \mathrm{d} * \mathrm{w} \quad (3)$$

d = flow depth (m) is assumed to be equal to direct run-off depth

w = grid cell size (30 m)

P= Wet perimeter (m)

Wet perimeter is the length of the grid boundary in contact with water

$$\mathrm{P} = \mathrm{w} + 2\mathrm{d} \quad (4)$$

Where w is the grid cell size and d is the flow depth

2.8.2.3. Travel time grid

Runoff takes various durations to pass through different areas of the basin. Travel time is defined as the time taken for a water drop to travel from one location within the watershed to another (Wong, 2001). It is possible to calculate the travel time between two specified sites using the following formula:

$$\mathrm{T_t} = \frac{\mathrm{L}}{60\mathrm{V}} \quad (5)$$

Tt = Travel time (hours-minutes)

L = Length or distance traveled (kilometer-meter)

V = Velocity or speed of flow (m/s)

60 = Factor converts velocity into a compatible unit for travel time calculation.

2.8.2.4. The time of concentration (Tc)

Represents the total time water needs to travel across the most distant watershed region before leaving through its outlet. During precipitation, runoff needs to travel the entire drainage basin distance to reach the outlet, which determines the Time of Concentration value. (Grimaldi et al., 2012).

$$\mathrm{t_c} = \frac{L^{0.8}[(1000/CN) - 9]^{0.7}}{1140S^{0.5}} \quad (6)$$

tc = time of concentration (hr)

L = longest path of flow, the distance between the hydraulically most remote point to the basin outlet, ft.

S = avg slope of certain watershed, CN = curve number, 1140 = constant

Lag time (Tl)

Hydrological parameter primarily used to determine the duration of flood events. It indicates the rate at which a watershed drains water after rainfall. Theoretically, lag time is closely related to the Time of Concentration (Tc). (SERBIULA, 1972)

$$\mathrm{T}_l = 0.6\, T_c \quad (7)$$

Tl = lag time (hour – minutes)

Tc = time of concentration (hour–minutes)

2.8.2.5. Flow routing using DEM

The process of flow routing includes identifying water transport routes as well as measuring the aggregate water amounts from every cell draining towards the outlet. Runoff data is placed on top of the flow direction grid for tracing water movement through drainage routes.

The integration of flow accumulation grids and runoff grids allows for estimating outlet runoff totals. Each rainfall cell within the routed runoff grid shows its accumulated volume of water and all runoff amounts gained from upstream cells.

2.8.2.6. Calculating total runoff

A combination of all upstream cell runoff values from the flow accumulation grid enables the determination of outlet runoff totals. This involves the flow accumulation grid being merged with the routed runoff grid for calculation; then the procedure for calculating cumulative runoff involves multiplying flow accumulation values from within the same grid cell to accumulate runoff from all upstream cells.

3. Results and Discussion

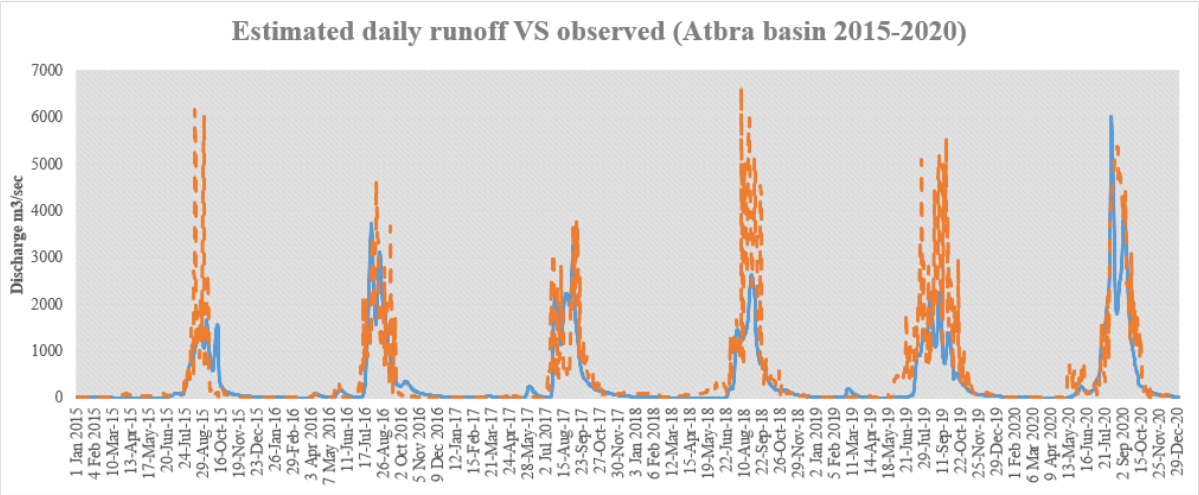


Fig. 14. Estimated daily runoff VS observed at Atbra-Tekezi basin outlet (2015-2020)

Fig. 14 illustrates the relation between estimated daily discharge and the observed daily discharge for the Atbara Basin for the period from 2015 to 2020. They are essential in viewing the efficiency and reliability of the hydrologic model applied in measuring river discharge.

3.1. Patterns and Trends

The seasonal variation in runoff strength appears similarly in estimated and observed results. The hydrologic model demonstrates appropriate timing in replicating the runoff events. The model shows signs of possible incorrect estimation through its estimated discharge output during the 2016 and 2019 periods, and it performed well at duplicating observed runoff patterns, making it efficient at handling seasonal runoff behaviors. The model shows potential for enhancement based on its deviations in particular years (2018-2020). Some limitations were noticed during peak discharge measurements and low flow periods because estimated values differ from observed data. Fig. 15 shows the average estimated runoff and average observed runoff over the period 2015-2020.

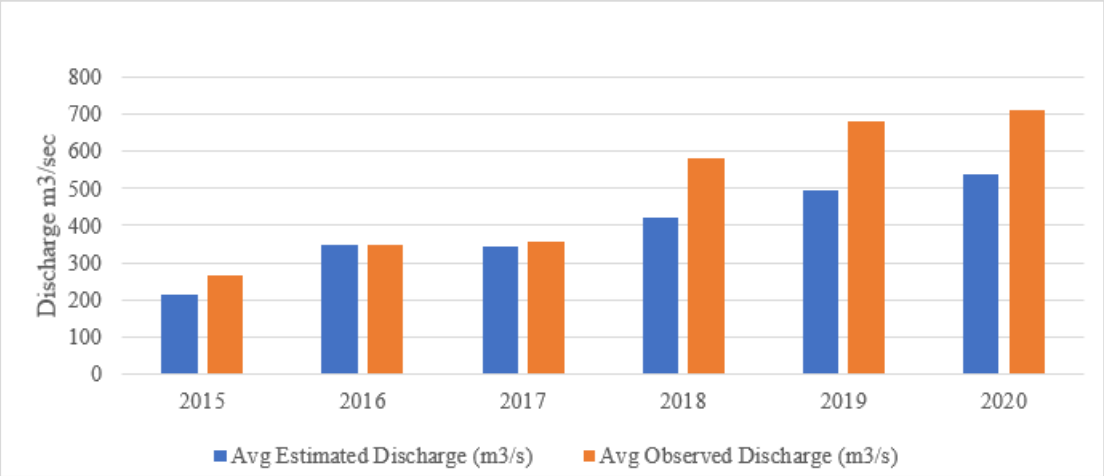


Fig. 15. Average annual estimated runoff VS observed at Atbra-Tekezi basin outlet (2015-2020)

In the year 2015, the observed runoff was higher than estimated, attributed to the discrepancy in this year. During 2016-2017, the estimated and observed runoff are very close to each other, highlighting good performance for the model for these years. From 2018 to 2020, the estimated runoff better aligns with the observed runoff; however, underestimation is still apparent.

3.2. Model Performance

The model seems to perform optimally in 2016 and 2017, having the smallest disparity between estimated and observed runoff. The analysis showed that there is a serious underestimation of the estimated runoff, especially during the high-discharge years (2018 to 2020).

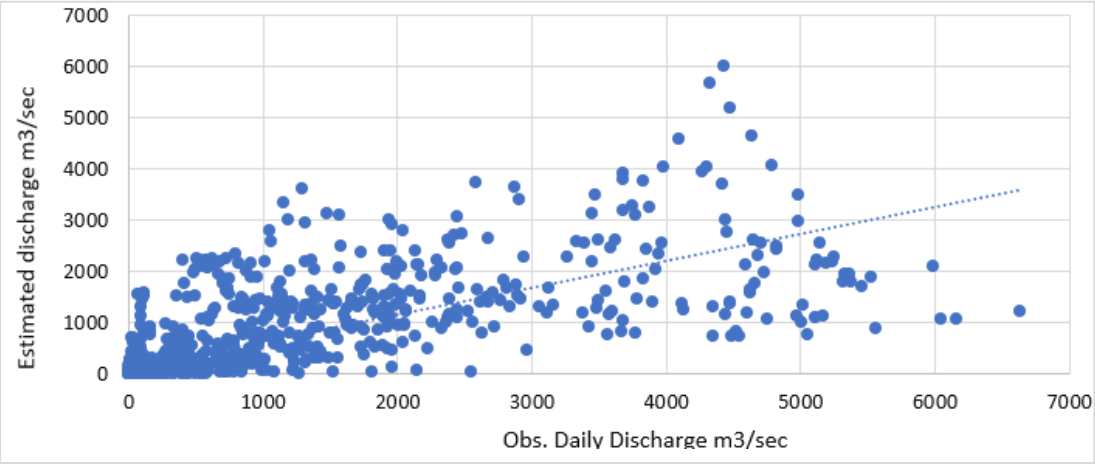


Fig. 16. Estimated daily runoff VS observed at Atbra-Tekezi basin outlet (2015-2020)

As shown in Fig. 16 results indicate a strong positive relationship stands between estimated and observed runoff data. The extent of regression line dispersion shows variations occurring during heavy runoff discharges

For the low to moderate runoff events (Runoff <2000 m3/sec), the model provides a reasonable estimation because sites cluster tightly together. And for the high runoff events (Runoff >3000 m3/sec): The model produces estimates which consistently fall beneath the trend line while numerous observations exist below this line indicating the model couldn't recognize notable events adequately.

The analysis of performance measures metrics (Corr., R2, PB, EFF, KGE) values of estimated and observed runoff are shown in Fig. 17.

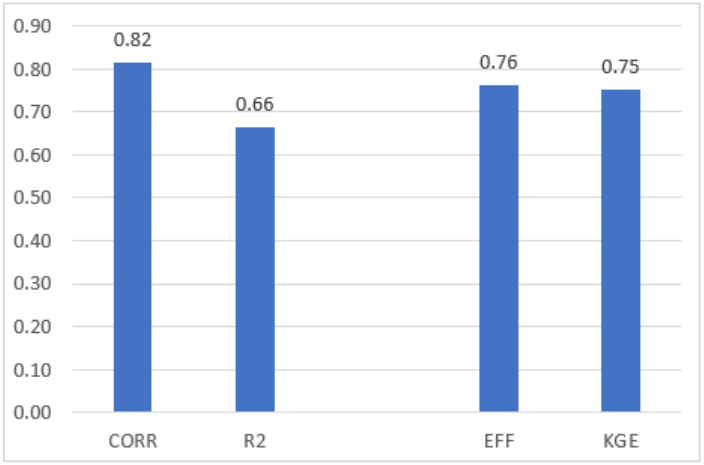


Fig. 17. Performance measures metrics (Corr., R2, PB, EFF, KGE) of estimated run-off VS observed at Atbra-Tekezi basin outlet (2015-2020)

The model shows a strong ability to estimate runoff since its correlation coefficient measures at 0.82. The model describes 66% of observed runoff changes ($R^2 = 0.66$) yet various uncertainties restrict its ability to interpret all variations. The pressure distribution accuracy of the model shows good results through an Efficiency Coefficient value of 0.76 while needing additional improvements when facing extreme runoff situations. The Kling-Gupta Efficiency rating of 0.75 points to an acceptable fit between estimated and observed runoff data. The results highlight that the model requires additional calibration procedures to reach output optimization which will establish better accuracy in observed versus predicted runoff metrics.

3.3. Model Calibration and Validation

The model was calibrated and validated using observed outflow data that were available for this study. Whereas the calibration period extends from 2015 to 2020, the validation period covers 2021 to 2024. The calibration process involved changing parameters of runoff coefficients to minimize the errors in the extreme event prediction.

- Manning roughness coefficient:

Since most of the discrepancies in the model were noted in high runoff events. Two input data for the manning roughness coefficient grid were fed to the model: one in the dry condition season in the Atbra-Tekezi basin from November to June and the other in the wet condition from July to October.as shown in Fig. 18.

Fig. 19 shows the estimated and observed daily flow in calibration and validation periods. The results show that the model corresponds well with the hydrologic cycle in both the calibration and validation periods. The accuracy in estimating run-off suggests the model effectively captures the long-term hydrological behavior for the basin outlet.

Before calibration, the model underestimated peak runoff events with lower performance metrics (CORR = 0.82, $R^2 = 0.66$, NSE = 0.76, KGE = 0.75). After calibration (2015–2020), adjustments to Manning's roughness coefficient improved accuracy, with metrics improved to CORR = 0.94, $R^2 = 0.88$, NSE = 0.87, and KGE = 0.98. In the validation period (2021-2024), the model showed a reliable efficiency, but its accuracy decreased, scoring a CORR of 0.91 with an R^2 of 0.83. The performance metrics for calibration and validation periods are shown in Table 2

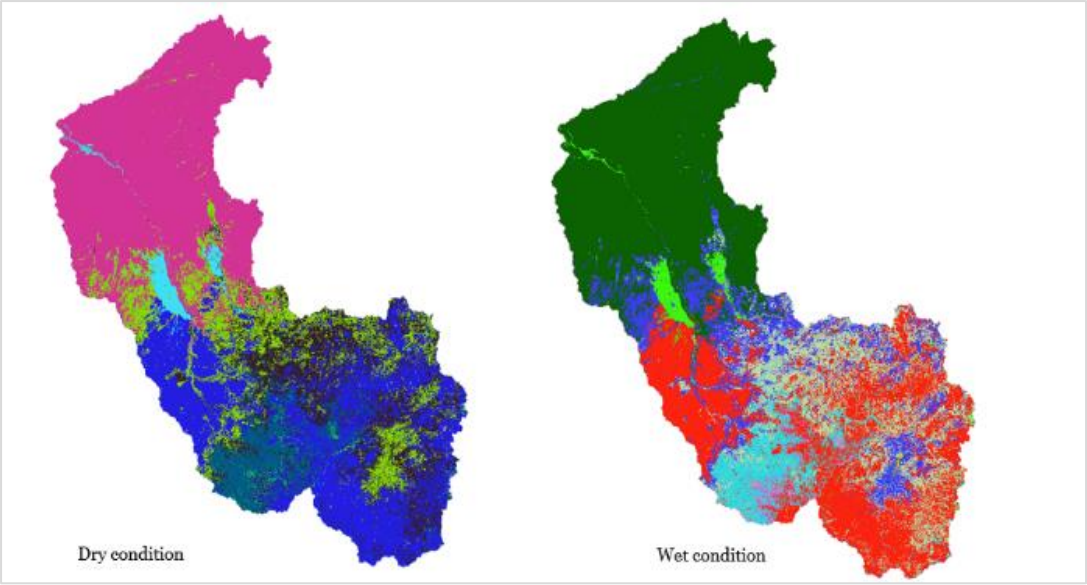


Fig. 18. Manning roughness coefficient gird for Atbra-Tekezi basin in dry and wet seasons

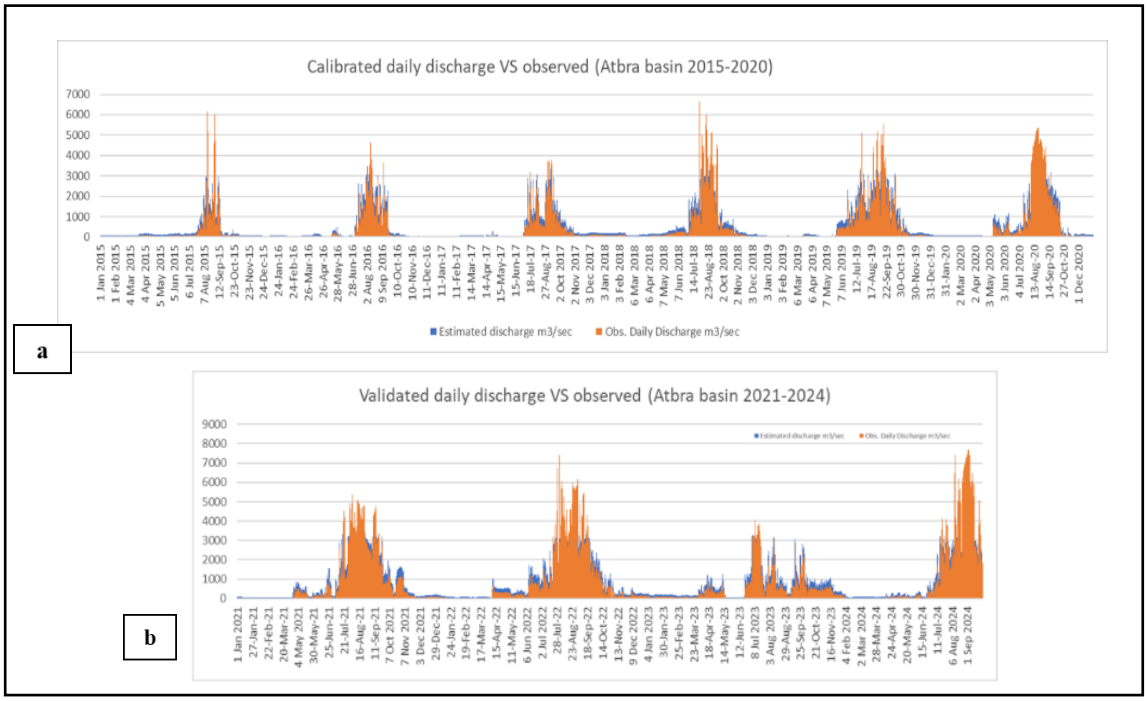


Fig. 19. Daily observed and estimated outflow from Atbra-Tekezi basin outlet: (a) calibration; (b) validation periods

Table 2. Model performance metrics in the calibration and validation periods.

Perforance Metric	Calibration Period (2015–2020)	Validation Period (2021–2024)
CORR (Correlation Coefficient)	0.94	0.91
R^2 (Coefficient of Determination)	0.88	0.83
EFF (Nash-Sutcliffe Efficiency)	0.87	0.82
KGE (Kling-Gupta Efficiency)	0.98	0.93

Model uncertainty emerges from several factors that include imprecise or scarce rainfall and soil moisture and land use and land cover data and simplified NRCS-CN method applications and assumptions during surface parameterization of Manning's roughness coefficient. According to the results high correlation values (e.g. CORR = 0.94 during calibration) did not eliminate the incorrect prediction of runoff during extreme events which demonstrated uncertain peak discharge measurement. The model displays sensitivity to calibration decisions and input parameter changes because it shows lower accuracy in measuring flows between 2018 and 2020 and inconsistent results from 2021 to 2024 model validation. The daily predictability of models requires frequent validation tests together with robust hydrological parameters and enriched datasets which should also include validation methods for model calibration.

4. Conclusions

The study successfully delivered a Cloud-Based Computational Model (CBCM), which uses remote sensing products and the NRCS-CN method to estimate direct surface runoff. The model was applied to the Tekeze-Atbara sub-basin in Sudan because the area faces difficulties using traditional runoff methods due to its arid and semi-arid climate conditions. The developed model combined Google Earth Engine (GEE) with GIS-based model builder to provide an effective tool for estimating real-time runoff calculations best suited for data-shortage areas.

The predictive capabilities of the developed model showed strong, accurate estimation capacities through a 0.82 correlation between predicted and observed runoff, then extended to 0.94 levels after adjusting parameter values. The model achieved its best performance by accurately predicting seasonal runoff throughout the period from 2016 through 2017.

Manning's roughness coefficient adjustments reduced underestimation errors detected during the extreme runoff events of 2018-2020. Testing confirmed that the model delivers valuable efficiency metrics (NSE = 0.87) and KGE = 0.98 after parameter adjustment, which demonstrates its capability to help water resource management.

The CBCM demonstrates robust predictive ability and flexibility when operating in dry and tropical areas of the Tekeze-Atbara sub-basin. The combination of remote sensing data and GIS introduces the CBCM as a system that can provide accurate runoff predictions across locations without direct observational data. Robust testing demonstrates that the model has achieved exceptional NSE value of 0.87 and KGE value of 0.98 under different hydrological conditions.The model allows valuable practical applications in water resource management systems. The system provides relevant and prompt data which enables enhanced decision-making capabilities related to city planning infrastructure and supporting flood-response systems and distributing water resources sustainably. The model application can provide helpful insights which assist local authorities and policymakers in decision making enhancing the region's capacity to adapt to conditions of water stress and climate change.

Recommendations

The focus of future work needs to enhance both features and implementation scope of the CBCM. Future research should apply the model to study predicted climate changes through time while including sediment simulation methods to build improved hydrological simulation models. The CBCM system would benefit from integration with present water resource platforms so managers can make decisions instantly. The ongoing validation of the model across diverse geographical locations and environmental conditions should continue next to automation development for time-sensitive data processing and collaborations with local governments dedicated to incorporate the model into their planning systems for infrastructure policy decisions.

References

Afkril, M., Irawan, D.E., Mulyadi, E., Mulyono, S., 2020. A new algorithm for the grid cell-based runoff routing model based on travel time concept. Geosfera Indonesia, 5(2), 160–185. https://doi.org/10.19184/geosi.v5i2.17351

Ajmal, M., Khan, M.A., Khattak, M.S., Nasreen, S., 2016. Runoff estimation using the NRCS slope-adjusted curve number in mountainous watersheds. Journal of Irrigation and Drainage Engineering-ASCE. https://doi.org/10.1061/(ASCE)IR.1943-4774.0000998

Akol, R. Galla, S. Wanyonyi, 2016, The Nile Basin Water Resources Atlas, Nile Basin Initiative.

Akol, P.J., Mwesigwa, D., Mungereza, C., Golit, P., Turyatunga, E., 2016. The Nile Basin Water Resources Atlas. Nile Basin Initiative.

Ashenafi, A., Alemayehu, T.Fentahun, B., 2023. Assessment of the use of remotely sensed rainfall products for runoff simulation in the Upper Blue Nile Basin of Ethiopia. Journal of Ethiopian Engineers and Architects,1–9.

Bergström, H., Gustafsson, J, Rahmberg, M., 2000. The waterscape. Sweden: Ditt Tryckeri i Uppsala AB.

Ebrahimian, M., 2012. Application of NRCS-curve number method for runoff estimation in a mountainous watershed. Caspian Journal of Environmental Sciences, 10(2), 103–114.

El Abbas, Doka M. Ali, R. Munro, K. Kucera, 2017. Pedological characterization of the soils of Atbara and Gash Rivers Upper Atbara Project Area (Kassala State - Sudan). European Journal of Applied Sciences, 5(6), 45–52. https://doi.org/10.14738/AIVP.56.4148

El-Bendary, N.M., 2019. Rainfall-runoff modelling using remote sensing data for Eastern Nile Watershed. Cairo.

El-Mahdy, S.M., Ahmed, M.T., Musa, S., 2024. Enhancing flood prediction in East Africa through satellite-based modeling. Remote Sensing Applications: Society and Environment, 29, 101024. https://doi.org/10.2166/wst.2024.070

Elsheikh, R.F., Mohamed, Y.A., van Griensven, A., Bauwens, W., 2014. Hydrological modeling of the Blue Nile Basin using SWAT model and remote sensing data. Hydrological Processes, 28(2), 1177–1191.

Fischer, G. et al., 2022. Global agro-ecological zones. Rome: Food and Agriculture Organization (FAO).

Funk, C., Peterson, P., Landsfeld, M. et al., 2015. The climate hazards infrared precipitation with stations: A new environmental record for monitoring extremes, Scientific Data. https://doi.org/10.1038/sdata.2015.66

Gebremicael, T.G., Mohamed, Y.A., Betrie, G.D., van der Zaag, P., Teferi, E., 2017. Temporal and spatial changes of rainfall and streamflow in the Upper Tekeze–Atbara River Basin, Ethiopia. Hydrology and Earth System Sciences, 21, 2127–2142. https://doi.org/10.5194/hess-21-2127-2017

Grimaldi, S., Petroselli, A., Tauro, F., Porfiri, M. 2012. Time of concentration: a paradox in modern hydrology. Hydrological Sciences Journal, 57(2), 217–228. https://doi.org/10.1080/02626667.2011.644244

Gupta, H.V., Kling, H., Yilmaz, K.K., Martinez, G.F., 2022. Decomposition of the mean squared error and NSE performance criteria: Implications for improving hydrological modeling. Water Resources Research, 58(4), e2021WR031543.https://doi.org/10.1080/17445647.2022.2076624

Jonathan, I. Green, E. James Nelson, 2002. Calculation of time of concentration for hydrologic design and analysis using geographic information system vector objects. Journal of Hydroinformatics, 4(2), 75–81. https://doi.org/10.2166/hydro.2002.0009

Kencanawati, R.N., El-Mahdy, S.M., Mohammednoor, A.E., 2024. Integrating Google Earth Engine and hydrologic models for runoff estimation in data-scarce regions. Environmental Modelling & Software, 167, 105595.https://doi.org/10.18517/ijaseit.14.2.19810

Miller, S., 1994. Measurement of runoff. In: Handbook for Agrohydrology. UK: Natural Resources Institute.

Mohammednoor, A.E., Elsheikh, R.F., El-Mahdy, S.M., Kencanawati, R.N., 2023. Development of a Cloud-Based Computational Model (CBCM) for runoff estimation in arid and semi-arid regions using remote sensing and GIS tools. Journal of Hydrology and Earth System Sciences, 27(5), 1234–1249. https://doi.org/10.1002/jqs.3574

Northern Illinois University, 2024. Climate Data from WMO Stations. Available at: https://atlas.niu.edu/

Nile Basin Initiative (NBI), 2016. Nile Basin Water Resources Atlas. Uganda: NBI.

Pal, B., Sinha, S.S., 2011. Surface runoff estimation and mapping using remote sensing and geographic information system. International Journal of Advances in Science and Technology, 3(2), 106–130.

Paudel, M., 2010. An examination of distributed hydrologic modeling methods as compared with traditional lumped parameter approaches. MSc thesis, Brigham Young University, Provo, USA.

United States Department of Agriculture (USDA), 1972. National Engineering Handbook, Section 4: Hydrology. Washington, DC: Soil Conservation Service.

Wong, T.S., 2001. Formulas for time of travel in channel with upstream inflow. Journal of Hydrologic Engineering, 6 (5), 416–422. https://doi.org/10.1061/(ASCE)1084-0699(2001)6:5(416)

Zhang, W. Y. , 2019. Application of NRCS-CN method for estimation of watershed runoff and disaster risk. Geomatics, Natural Hazards and Risk, 10(1), 2220–2238. https://doi.org/10.1080/19475705.2019.1686431